2011 17th IEEE Real-Time and Embedded Technology and Applications Symposium

Ultra Low Power Granular Decision Making using Cross Correlation: Optimizing Bit Resolution for Template Matching

Hassan Ghasemzadeh, Roozbeh Jafari
Embedded Systems and Signal Processing Lab
Department of Electrical Engineering
Univeristy of Texas at Dallas, Richardson, TX 75080–3021
Email: {h.ghasemzadeh, rjafari}@utdallas.edu

***Abstract*—Advances in technology have led to development of wearable sensing, computing and communication devices that can be woven into the physical environment of our daily lives, enabling a large variety of new applications in several domains including wellness and health care. Despite their tremendous potential to impact our lives, wearable health monitoring systems face a number of hurdles to become a reality. The enabling processors and architectures demand a large amount of energy, requiring sizable batteries. In this paper, we propose a granular decision making architecture that can be viewed as a tiered wake up circuitry. This module, in combination with a low-power microcontroller, enables an ultra low-power architecture. The significant power saving is achieved by performing a preliminary ultra low-power signal processing and hence, keeping the microcontroller off when the incoming signal is not of interest. The preliminary signal processing is performed by a set of special purpose functional units, also called screening blocks, that implements template matching functions. We formulate and solve an optimization problem to select screening blocks such that the accuracy requirements of the signal processing are accommodated while the total power is minimized. Our experimental results on real data from wearable motion sensors show that the proposed algorithm achieves 65.2% energy saving while maintaining 92.7% sensitivity in recognizing human movements.**

***Keywords*-Medical Embedded Systems; Body Sensor Networks; Signal Processing; Power Optimization.**

I. Introduction

Long-term pervasive sensing and monitoring can aid in diagnosis and tracking of certain diseases such as Parkinson's [1] or extracting biokinematic characteristics of human body such as gait parameters [2]. Advances in technology have led to development of wearable sensing, computing and communication devices that can be woven into the physical environment of our daily lives, enabling a large variety of new applications in several domains including wellness and health care. These systems, also called Body Sensor Networks (BSNs), enable real-time monitoring of the human body. A BSN consists of several nodes placed on the human body that provide sensing, processing and communication capabilities. BSNs offer the unprecedented ability to monitor patients in a natural setting for an extended period of time.

Despite their tremendous potential to impact our lives, wearable health monitoring systems face a number of hurdles to become a reality. The enabling processors and architectures demand a large amount of energy, requiring sizable batteries. This creates challenges for further miniaturization of the wearable units.

This paper introduces an ultra low-power *granular decision making* methodology based on coarse to fine grained signal processing techniques requiring low to slightly higher power. This architecture is presented in the context of physical movement monitoring which aims at detecting a target human action such as 'walking', 'sit to stand', 'kneeling', or 'lie to sit'. The granular decision making module (GDMM) will remove actions that are *not of interest* as early as possible from the signal processing chain, deactivating all remaining signal processing modules, including the microcontroller. The granular decision making module can be viewed as a tiered wake up circuitry. It is composed of hundreds or thousands of choices of screening blocks, although in this paper, we consider only a specific case where bit resolution of sensor readings is considered for optimizing power consumption of decision making architecture. Each screening block is essentially a classifier with several tunable parameters, by which power versus classification accuracy can be adjusted.

Emerging applications of health care monitoring have unique properties motivating the proposed research: signals and events observed from the human body are slowly changing. They are governed by the physics of the human body (e.g. kinematics, dynamics) which constrains the variations and reduces the randomness in the signals. In addition, *events of interest*, which may require the microcontroller's attention, often occur with a low duty cycle [3]. We exploit theses properties to propose novel programmable multi-level information driven decision making techniques that are highly power optimized.

The contributions of this paper can be summarized as follows: 1) we present a novel programmable architecture for detecting low duty cycle actions mainly for physical movement monitoring, 2) we first model the signal processing tightly with the architecture and HW and then propose an optimization problem for minimizing the number of functional units used for preliminary signal processing, 3)

1080-1812/11 $26.00 © 2011 IEEE
DOI 10.1109/RTAS.2011.21

we propose algorithms for solving the optimization problem and present experimental results on real data collected from our BSN platform and demonstrate the energy efficiency of the proposed granular decision making architecture.

II. Related Works

Several ultra low-power wearable systems, with power budget of less than 1 mW, with signal processing capabilities have been proposed. The proposed systems, however, are either not programmable (except that they may provide a few tunable parameters), or the programmability is handled completely by a microcontroller. An intraocular CMOS pressure sensor system implant was proposed which contains an on-chip micro mechanical pressure sensor array, a temperature sensor, a microcontroller-based digital control unit, and an RF transponder [4]. An interface chip for implantable neural recording was proposed with tunable band-pass filters and adjustable gain [5]. A battery-less accelerometer system, with 3D loop antenna, was proposed that utilizes the radio wave for power feeding and signal communication as RFID. However, the control unit of the system is a microcontroller and is unclear how it can be powered up by energy scavenging [6].

Several other systems were suggested that are primarily tailored towards specific applications and are not generalizable. Examples include a machine-learning based patient-specific seizure detector [7], an implantable blood pressure, ECG sensing micro-system with adaptive RF powering [8–11], an implantable battery-less telemetric micro-system for EMG recording [12] and a battery-less MEMS implant for cardiovascular applications [13].

There has been some effort towards creating ultra low-power semiconductor components. Multi-threshold CMOS (MTCMOS) circuits is an example [14]. A wireless system with MTCMOS/SOI circuit technology was suggested which lowers the supply voltage of the LSIs 0.5 V and reduces the power dissipation to 1 mW [15]. 1 mW, however, is still larger than the energy budget of the energy harvesting circuits. The power budget of energy harvesting circuits is often tens of μWs. For example, a battery-less vibration-based energy harvesting system was proposed for ultra low-power ubiquitous applications that can generated 36.79 μW [16].

Our approach is different from previous works: 1) our granular decision making module is composed of extremely low-power functional units that perform template matching on incoming signals, 2) the proposed architecture takes into account specific properties of BSN applications and their signal processing requirements, 3) our signal screening module is reprogrammable in the sense that it can be embedded with the microcontroller to provide signal screening for monitoring low duty cycle events.

Table I
Notations

Term	Description
BSN	Body Sensor Network
GDMM	Granular Decision Making Module
MSPC	Main Signal Processing Chain
MCSP	Minimum Cost Screening Path
$\hat{a}$	target action
A	set of m not-target actions
T	template generated for target action $\hat{a}$
$\gamma(T,S)$	similarity score between template T and signal segment S
n	maximum number of quantization bits provided by ADC
B_i	i-th screening block
thr_i	threshold value for screening block B_i
b_i	bit resolution of screening block B_i
tp_i	true positive rate, percentage of target actions accepted by B_i
fp_i	false positive rate, percentage of non-target actions accepted by B_i
F	desired true positive rate
w_i	per-action energy consumption of B_i

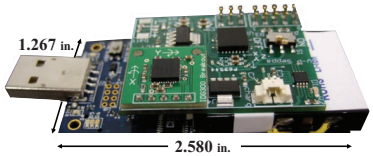

Figure 1. A sensor node with two sensor modalities (accelerometer & gyroscope), microcontroller, radio, and battery.

III. Preliminaries

The problem addressed by this paper is energy savings in BSNs through a preliminary signal screening block, called granular decision making module. Before presenting more details of our ultra low-power architecture, we present major components of a typical BSN platform including sensing hardware and signal processing flow. Throughout this paper, we use notations listed in Table I.

A. Sensing Platform

A BSN is composed of several sensor nodes mounted on the patient's body, embedded with the clothing, or implanted in the human body [17]. Figure 1 shows a sensor node that can be attached to the patient's body for motion analysis. Physical movement monitoring uses inertial information acquired by motion sensors such as accelerometers, gyroscopes, and magnetometers. The sensor node also has a processing unit, TelosB mote [18], with several analog-to-digital (ADC) channels responsible for acquiring and digitizing analog signals for further analysis. The MSP420 microcontroller used for our experiments has an ADC unit of 12-bit resolution. The sensor node has also a radio module for communication with other nodes in the network or with a gateway such as a cell phone. Note that our 'Sensing Platform' is purely used for data collection. In Section VI, the data collected from this platform will be used to validate the architecture presented in Section IV-B.

Figure 2. MSPC (Main Signal Processing Chain) for action recognition.

B. Main Signal Processing Chain

The goal of main signal processing chain (MSPC) is to extract useful information from sensor data [19]. Frequently, this data is a high-level observation, such as "Is the subject running?" or "What is the stride length when the subject is walking?". In other words, the purpose of main signal processing is to provide a 'fully' SW programmable environment for development of 'highly' reliable signal processing techniques for action detection/verification and extracting details from the signals (e.g. balance during 'sit to stand' when it occurs).

In many cases, out of all possible actions, only a few are of interest to the main signal processing (e.g. 'walking' or 'sit to stand'). Therefore, the main signal processing needs to classify actions of interest prior to extracting any further details about actions. The overall goal of classifier is labeling actions of interest, also called target actions. Figure 2 shows a typical signal processing model commonly used for movement monitoring applications [20]. In this model, signals are processed in real time by a series of processing blocks to arrive at a classification result. These processing blocks include filtering, segmentation, feature extraction, and classification and parameter extraction. The filtering is generally applied to remove sensor artifacts and noise. In the context of action recognition, segmentation determines portions of the signal that represents a complete action, segregating activity versus rest. Features are functions run on the segmented data to decrease dimensionality of the signal without significantly reducing the relevant information. Statistical features are frequently used for action recognition [21]. Finally, each node uses the feature vector generated during feature extraction to determine the most likely action by utilizing some classification algorithm such as k-Nearest Neighbor (k-NN) [22].

IV. Screening Approach for Power Saving

This section presents different components of our energy-efficient architecture. We describe motivation for signal screening first, and present a top level view of our system followed by more detailed information on each component of the system in subsequent sections.

A. Motivation

Most BSN applications are only concerned with a very small subset of human actions. For instance, gait analysis only is concerned with 'walking', fall detection with 'falls', Parkinson's disease monitoring with certain movements such as 'tremors' [23], sleep apnea with 'restless leg syndrome' and 'periodic limb movements' [24]. In real-time continuous patient monitoring, these target actions occur infrequently. Considerable energy is wasted processing non-target actions. As a result, efficiently rejecting non-target actions with a screening classifier could lead to a significant increase in system lifetime through deactivating the main processor which provides the full signal processing for classification. This way, an ultra low-power screening block activates the MSPC only when a target action is observed. Clearly, one requirement of such screening classifier is to achieve a significantly high sensitivity, *true positive rate*, in detecting target actions (activating main processor due to occurrence of a target action). To obtain high true positive rates, the screening architecture may accept some non-target actions. Such actions determine the *false positive rate*. For the actions that the screening block cannot reject reliably, the MSPC will be activated. The main advantage of this method is the power saving due to removing non-target actions from the signal processing chain, deactivating the remaining modules in the signal processing chain. We note that the false positives may not generate problems as they can be reliably detected by MSPC.

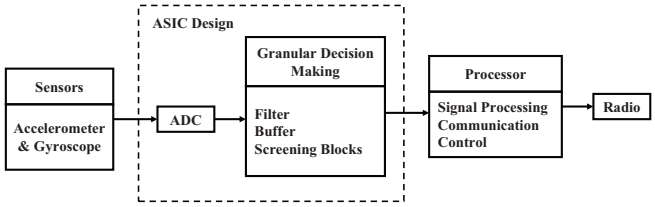

Figure 3. Architecture of proposed system with GDMM.

B. System Architecture

An overview of our system architecture for low-power signal processing is shown in Figure 3. There are four main portions of the platform: the sensors, the proposed special purpose functional unit or granular decision making module (GDMM), a low-power general purpose processor, and the radio. Human actions can be examined using motion sensors such as accelerometers and gyroscopes. The sensor readings are sent through an ASIC architecture including an analog-to-digital converter (ADC) and GDMM, which digitizes the reading and performs screening tests. The ADC is an essential component which acquires and digitizes analog signals for further analysis. The MSP420 microcontroller used for our experiments has an ADC unit with 12-bit resolution. Any action that is accepted by the GDMM will be forwarded to the MSPC for further processing. The MSPC presented in Section III-B is implemented on the main processor where the results can be transmitted through the radio.

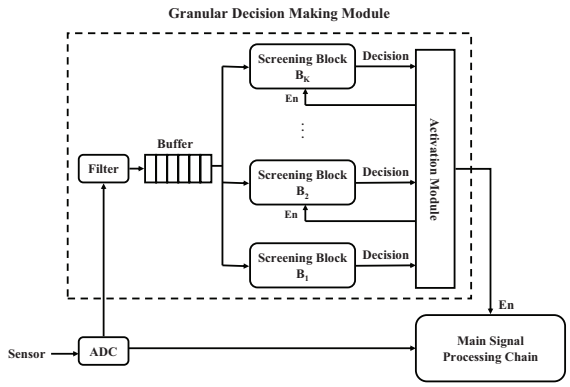

Figure 4. GDMM (Granular Decision Making Module) composed of several screening blocks, each having a different bit resolution.

C. Granular Decision Making Module

Our power saving model is based on a set of screening blocks performing template matching on incoming signal. Each screening block can be turned on to perform preliminary signal processing at different true positive rates at the cost of power usage. An example of tunable parameters is the number of quantization bits or bit resolution of the sampled data. Specifically, optimizing the screening architecture with respect to bit resolution is the main focus of this paper. Figure 4 illustrates GDMM in connection with other components of the system where screening blocks operate at different bit levels. The module includes digital pre-filtering, a buffer, and a chain of screening classifiers as described previously. The sensor data from body-mounted motion sensors is frequently noisy. A moving average filer is enough to filter the signal and remove high frequency noise [25].

As discussed before, each screening block in the chain is applied in a sequence that will be detailed in Section V. The processing stops as soon as a screening block in the chain rejects the incoming action. Activating screening blocks in serial introduces a time delay for each subsequent block. In order to allow each block to operate on the proper signal segment, a single buffer is used.

The lowest level screening block (i.e. B_1) has the lowest sensitivity rate due to the low resolution (e.g. 1-bit) but is also the least energy consuming block. An active screening block makes a preliminary binary decision (Accept/Reject) on incoming signal. A higher level block (e.g. B_2) is activated only if the incoming action is accepted by the preceding block (e.g. B_1). Clearly, the block at the lowest processing level (e.g. B_1) needs to be active all the time. In Section V, we present an optimization problem aiming to find the optimal sequence of the screening blocks where quantization bit is considered as the tuning parameter.

The *Activation Module* is responsible for turning on the next screening block or the MSPC. That is, activation of the screening blocks and the main processor are programmable thought the activation module. A higher-level screening block is activated only if the current action is accepted by its preceding block.

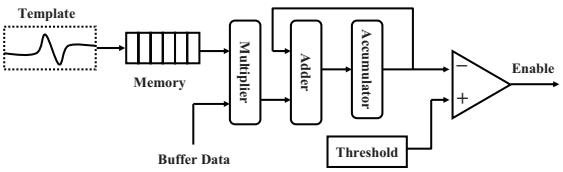

Figure 5. Screening block performing template matching operations.

D. Screening Blocks

Each screening block compares the incoming signal against a predefined template over a fixed window. The comparison is made using template matching operations. The template matching is based on Normalized Cross Correlation (NCC) [26] which will be discussed in Section V-A. Template matching is implemented using a multiplier-accumulator (MAC) circuit as shown in Figure 5.

Each screening block is a binary template classifier based on the cross correlation score obtained by comparing the incoming action with a pre-computed template of the target action. This comparison assigns a score value, γ, based on the similarity between the signal segment and the template. For classification decision, γ is compared against a threshold value, thr_i, and the action is classified as either *accept* or *reject*. A rejection causes processing to stop for that action.

V. Minimum Cost Screening Path

The GDMM in Figure 4 is composed of several screening blocks that form a decision path for classification. Each block is associated with a quantization bit level which affects performance of the classification. Finding minimum set of screening blocks and their ordering is challenging because each block has a different operating point depending on the bit resolution and the threshold used for classification. In this section, we formulate an optimization problem in order to find the optimal decision path forming the best sequence of screening blocks for examining each incoming action.

A. Template Matching

Given a target action $\hat{a}$ and a set of m non-target actions, $A = \{a_1, a_2, \ldots, a_m\}$, we generate template T, associated with $\hat{a}$, from a set of training trials. Templates are generated as shown in Definition 1 using a set of training trials. During real-time operation of the system, a classification decision is made by comparing the incoming action to the predefined template. The comparison is made based on the similarity score defined in Definition 2.

***Definition** 1 (Template):* Given a target action $\hat{a}$ with L number of training trials, a template T for $\hat{a}$ is generate by averaging the entire set of training trials.

***Definition** 2 (Similarity Score):* Given two time series signals f and g of length N, the similarity score $\gamma(f,g)$ between the two signals is defined based on their normalized cross correlation by

$$\gamma(f,g) = \frac{\sum_{t=1}^{N}[f(t)-\bar{f}][g(t)-\bar{g}]}{\sqrt{\sum_{t=1}^{N}[f(t)-\bar{f}]^2 \sum_{t=1}^{N}[g-\bar{g}]^2}} \quad (1)$$

where $\bar{f}$ and $\bar{g}$ denote mean values of f and g.

B. Performance of Screening Blocks

As mentioned previously, each screening block performs preliminary classification based on the score associated with cross correlation between the template and the incoming action. A screening block B_i rejects the incoming action if the score is smaller than a certain threshold thr_i. Classification performance of a screening block B_i depends on thr_i and the bit resolution of the block, b_i. The threshold is set during the training to obtain a pre-specified accuracy associated with a desired performance criterion. The larger the threshold is, the higher the likelihood of rejecting an incoming action. Therefore, the threshold value directly affects the true positive rates (tp_i) and false positive rates (fp_i). Our granular decision making architecture aims to minimize power consumption of the system while maintaining a given lower bound on the true positive rate (F). The module introduces a decision path including a sequence of the screening blocks. The power consumption of the module is determined by the *acceptance rate* of the screening blocks on the path (r_i) and the energy consumption of each block (w_i). We call this problem *Minimum Cost Screening Path* (MCSP) and study this problem by mapping the entire set of screening paths onto a graph model and formally formulating the problem on the proposed graph.

***Definition** 3 (Block Acceptance Rate):* For each screening block B_i on a decision path, an acceptance rate r_i is defined by

$$r_i = tp_i + fp_i \quad (2)$$

where tp_i and fp_i refer to true positive rate and false positive rate of the block B_i. The acceptance rate r_i is clearly determining percentage of the actions (including target and non-target) accepted by B_i.

C. Problem Formulation

In order to present the minimum cost screening path (MCSP) problem, we first map all possible decision paths onto a graph model called *screening graph*. We then use this model to find the optimal path including a subset of screening blocks and their ordering for preliminary signal screening.

***Definition** 4 (Screening Graph):* Given a set of screening blocks $\{B_1, \ldots, B_n\}$ with $b_i < b_{i+1}$, the screening graph G=$\{V,E, R,W\}$ is a directed acyclic graph defined by a set of vertices, V, a set of edges, E, and sets of weights, W, and outgoing rates, R, associated with the vertex set. The set of vertices, V, is $\{s, v_1, \ldots, v_n, t\}$ where s is a dummy node connected to all other nodes, and t is the sink node associated with the main signal processing chain. Thus, $|V|$=n+2. Furthermore, each vertex v_i ($1 \leq i \leq n$) is associated with a screening block B_i. An edge e_{ij} ($i < j$) connects a vertex v_i (corresponding to a lower level block B_i) to vertex v_j (corresponding to higher level block B_j). Thus, $|E|$=$\frac{(n+1)(n+2)}{2}$. The set W=$\{w_1, \ldots, w_n\}$ denotes cost of each vertex for processing a single incoming action, and is associated with the energy consumption of corresponding screening blocks. Moreover, the set R=$\{r_1, \ldots, r_n\}$ represents acceptance rates of corresponding screening blocks. In other words, r_i denotes percentage of actions that are accepted by B_i.

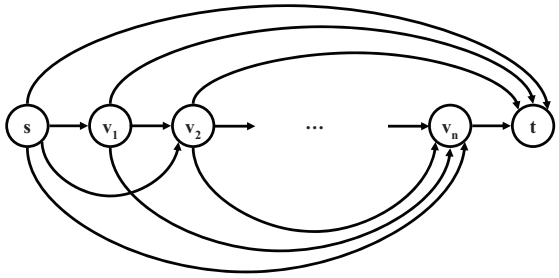

Figure 6. Screening graph

For the dummy node s, r_s=1 resulting in an acceptance rate of 1. The idea is to feed all actions to the dummy node first. A path from s to t determines active screening blocks during preliminary classification. Furthermore, w_s=0 because the dummy node does not represent a physical component of the system. We assign a zero outgoing rate to the destination node (r_t=0) because MSPC is the last processing component of the system and does not convey actions to any subsequent components. The energy consumption of the destination node, w_t, is calculated by the amount of energy required for running MSPC on the main processor.

Figure 6 shows the screening graph with v_1 to v_n corresponding to n screening blocks. As mentioned previously, the energy cost of a screening block B_i is denoted by w_i per incoming action. Therefore, the overall cost of each screening block depends on the percentage of the incoming actions that are passed through the decision path to the screening block B_i. This is directly defined by the acceptance rate of preceding blocks on the path. Thus, each path in the graph has a different cost. Our objective is to find the decision path with the minimum overall cost.

To better show how the overall cost for a path from s to t is calculated, we present a synthetic screening graph (Figure 7) with three screening blocks indicated by u_1, u_2, and u_3. Each vertex has an incoming rate, r_i and a weight denoted by w_i. The weights are shown in nW with

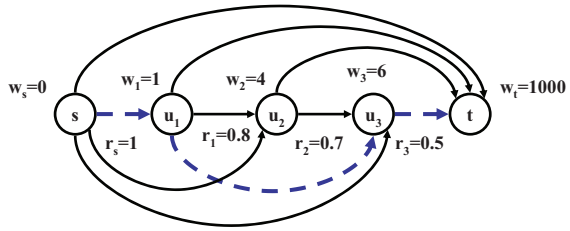

Figure 7. An example of a screening graph with four vertices. A minimum cost decision path is P=$\{s, u_1, u_3, t\}$ with a total cost of 505 nW.

destination node (t) having a significantly larger amount of power consumption (e.g. w_t=1000) as it corresponds to the main signal processing chain. A path P=$\{s, u_1, u_3, t\}$ which is the minimum cost path has a cost of 505 nW. The edge (s,u_1) has a cost of $r_s \times w_1$=1 nW. The next edge, (u_1,u_3) has a cost of $r_1 \times w_3$=4.8 nW. We note that, in fact, r_1 is the minimum rate among all previously traversed vertices (s and u_1). The cost for the edge (u_3,t) is $r_3 \times w_t$=500 nW. Similarly, r_t is the smallest rate among previously traversed nodes (s, u_1, u_3). In general, however, if r_i is not the smallest rate among all preceding nodes, the cost for an edge e_{ij} is a function of rates on all previously traversed nodes. In this example, acceptance rates are monotonically decreasing. Thus, the cost for each edge e_{ij} can be computed based on the rate and weight of adjacent vertices (i.e. r_i and w_j). In order to formally define the MCSP problem, we first define the cost for each decision path on a given screening graph.

***Definition** 5 (Decision Path Cost):* Given a screening graph G, the total cost of a decision path P=$\{s, u_1, \ldots, u_l, t\}$ of length l is given by

$$\mathbf{w}^P = r_s w_1 + min(r_s, r_1) w_2 + min(r_s, r_1, r_2) w_3 + \cdots + min(r_s, r_1, \ldots, r_l) w_t \quad (3)$$

where $u_i \in V$, r_i is the incoming rate for vertex u_i, and r_s=1. Furthermore, each term $min(r_s, r_1 \ldots, r_i) w_j$ represents the cost associated with the edge e_{ij}=(u_i,u_j) on the path.

As it can be observed from Definition 5, the cost for each edge e_{ij} on the path depends on the cost of u_j and acceptance rate of all previously traversed nodes.

***Problem** 1:* Given a screening graph G, the MCSP problem is to find a decision path, $\hat{P}$, with minimum cost.

$$\hat{P} = \arg\min_{P} \quad \mathbf{w}^P \quad (4)$$

***Definition** 6 (Path Acceptance Rate):* For a decision path P from s to t on the screening graph G, the acceptance rate R_P is defined as the percentage of actions that are accepted by all the node on the path, and is given by

$$R_P = min_{u_i \in P}(r_i) \quad (5)$$

D. Shortest Path Solution

The problem presented in Section V-C is different from the classical shortest path problem because the contribution of an edge to path cost depends not only on the cost of that edge but also on the costs of the edges already traversed. A special case of this problem with applications in multimedia data transmission has been studied in [27].

We transform the MCSP problem to the traditional shortest path by simplifying some of the assumptions on acceptance rate of our screening blocks. We show that under these realistic assumptions, the problem can be solved with typical shortest path algorithms (e.g. Dijkstra's algorithm [28]).

In our work, the classifiers use the same template and signal, but linearly quantized at different bit levels. From this model, several basic assumptions can be inferred.

1) The target actions are rejected in approximately the same order by all the screening blocks on the decision path. Equivalently, if a target action is rejected by B_i, it is also rejected by B_j while $j > i$. In other words, a higher level block B_j may reject some target actions that are accepted by B_i. Therefore, compared to a lower level block, a higher level block may have smaller or equal true positive rate ($tp_j \leq tp_i$).
2) Similarly, the non-target events are rejected in approximately the same order by all the classifiers. Thus, a higher level block B_j may reject some non-target actions that are accepted by a lowe leve block B_i. Therefore, compared to a lower level block, a higher level block may have smaller or equal false positive rate ($fp_j \leq fp_i$).
3) Classifiers at higher quantization bit levels perform better or equal to classifiers at lower bit levels. That is to say, for two screening blocks with equal true positive rates $tp_i = tp_j = F$ and $j > i$, $r_j \leq r_i$. In fact, in order to achieve the lower bound F on true positive rate of the entire granular decision making, we set the threshold thr_i on each screening block such that the minimum true positive rate of F is obtained.

***Theorem** 1:* If $u_1, u_2, \ldots, u_k$ (associated with screening blocks $B_1 \ldots B_k$) form an optimal decision path, the cost of an edge e_{ij} is a function of w_j and r_i.

Proof: As shown in (3), the total cost associated with edge e_{ij} on path P is given by

$$w^e_{ij} = min(r_s, r_1, \ldots, r_i) w_j \quad (6)$$

The assumptions on monotonically decreasing acceptance rate would result in u_i having smallest acceptance rate among all preceding nodes. That is $min(r_s, r_1, \ldots, r_i)$=$r_i$. Therefore,

$$w^e_{ij} = r_i w_j \quad (7)$$

■

The immediate result of Theorem 1 is that the cost of each edge on the decision path is deterministic and can be

Table II
EXPERIMENTAL ACTIONS

No.	Actions
1	Stand to sit
2	Sit to stand
3	Sit to lie
4	Lie to sit
5	Bend and grasp
6	Kneeling
7	Turn clockwise
8	Turn counter clockwise
9	Step forward
10	Step Backward

computed before running any algorithm for computing the path. Therefore, the problem is transformed into a simple shortest path problem [28].

VI. EXPERIMENTAL RESULTS

We evaluated performance of our granular decision making architecture for identifying each one of the 10 target actions listed in Table II. In each phase, one of the actions was considered as target action and the rest as non-target. A set of experiments was carried out on three male subjects, all between the ages of 25 and 35 and in good health condition. Subjects were asked to repeatedly perform each specific action ten times.

A. Data Acquisition Platform

Nine sensor nodes, each as shown in Figure 1, were used for data collection. Each sensor node had a 3-axis accelerometer, a 2-axis gyroscope. The data were collected and processed in MATLAB. For simplicity, we used only one sensor (Z-axis of the node placed one the 'waist'). For actions that require multiple sensors, the same methodology can be used. That is, the template matching on multiple nodes/axes can be utilized to activate MSPC. In this case, a data fusion algorithm will be used to combine decisions made by different sensors and decide if the microcontroller needs to be tuned on/off. The data fusion from multiple sensor nodes is out of scope of this paper (for brevity) and is the subject of our future work.

For the purpose of action recognition, we used the TelosB motes [18] which have an embedded MSP430 microcontroller, particularly used for executing main signal processing tasks, and consume 3 mW in active mode.

B. Template Generation

The sensor data recorded from each action were equally split into training and test datasets. The training dataset was used for template generation as well as construction of the optimal decision path, and the test dataset was used for validation of the results.

Table III
SHORTEST PATH AND POWER CONSUMPTION FOR DETECTING 'SIT TO STAND'.

Sensitivity (%)	Template Length (# of samples)	Bit Resolutions Used	Power (nW)
50	300	$1 \rightarrow 9$	5.68
60	300	$3 \rightarrow 9$	6.20
70	300	$3 \rightarrow 10$	6.64
80	300	$4 \rightarrow 10$	6.76
90	300	$4 \rightarrow 11$	6.84
95	300	$4 \rightarrow 11$	7.02

C. Parameter Setting

As discussed in Section V, a screening graph has two sets of parameters which are used for constructing optimal decision path. These parameters include weights (W) and incoming rates (R) associated with different screening blocks. Both parameters are calculated using training trials. Weights are calculated based on the amount of energy consumed by corresponding screening blocks. Incoming rates are calculated by examining percentage of training trials that are accepted by each screening block.

To estimate energy consumption of each screening block, the screening blocks were implemented using template matching units as described previously. Template matching function was modeled using Verilog. The cross-correlation was implemented by a series of MAC steps depending on the number of incoming samples. At each clock instant, the digitized template data and the incoming signal data were multiplied and added to the previous MAC value. The multiply-add operation repeated depending on the length of the template, to calculate the cross correlation function. All the operations were carried out at a low frequency of 20 Hz. The design was synthesized using Synopsys with the 45 nm NanGate Open Cell library. The switching activity was then considered and the power numbers were computed in Synopsys. The power consumption was computed by determining the switching activities of transistor. The power values ranged between 0.34 nW for the 1-bit block (w_1=0.34) and 1.45 nW for the 12-bit screening block (w_{12}=1.45).

In order to calculate the incoming rates (R) on individual vertices of the screening graph, we set the threshold (thr_i) on each screening block such that the desired true positive rate (F) is obtained. In fact, the threshold is set to guarantee the lower bound F on the overall sensitivity of the system. Therefore, the threshold on each screening block B_i is given by

$$\hat{thr}_i = \underset{thr_i}{\arg\min} \quad tp_i \geq F \tag{8}$$

We note that tp_i decrease as thr_i grows. Thus, thr_i is set to the smallest value that meets the desired sensitivity requirement.

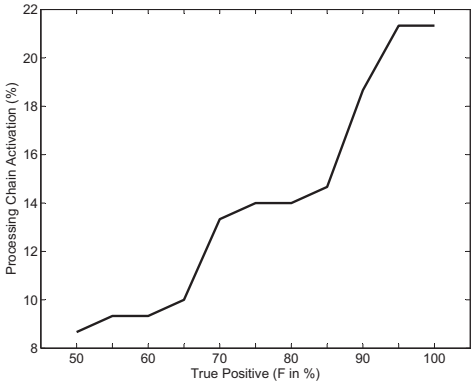

Figure 8. Path acceptance rate as a function of sensitivity, for detecting 'sit to stand'.

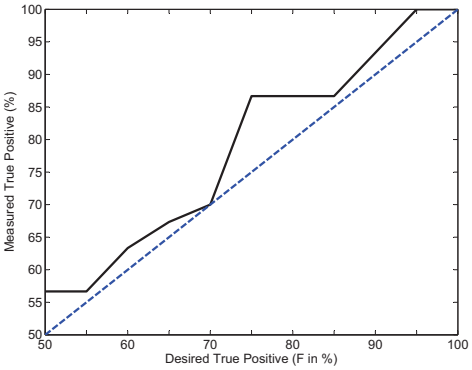

Figure 10. Comparing measured versus desired true positive rates when 'sit to stand' is target action. It shows percentage of the time that the main signal processing chain (MSPC) is active.

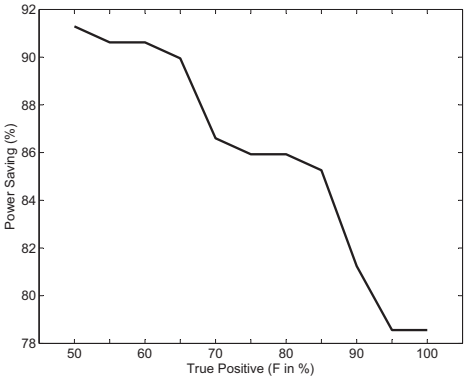

Figure 9. Power saving as a function of sensitivity, for detecting 'sit to stand' through the granular decision making module (GDMM).

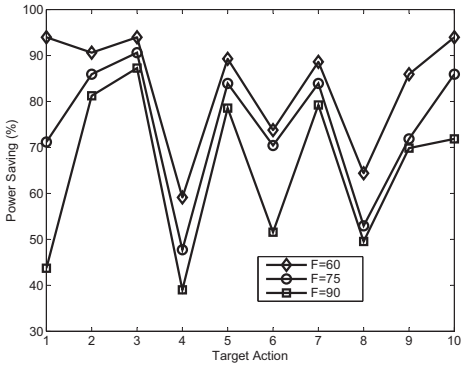

Figure 11. Power saving for detecting different movements. Results are shown for three values of desired true positive (60%, 75%, and 90%.).

D. Decision Path

Table III shows decision path reported by our optimization technique while the desired true positive rate (F) varies from 50% to 95%. In all cases, only two screening blocks are chosen by the algorithm. We note, however, that the total energy depends also on the bit resolution of the individual screening blocks. For example, B_{11} consumes more power than B_4. The third column in Table III shows path acceptance rate, percentage of the time that the main signal processing chain (MSPC) is activated by the algorithm. We note that the first screening block (e.g. 3-bit or 4-bit template matching blocks) is active all the time. However, the second screening block is activated based to the outcome of the previous template matching.

The power optimization problem with a desired true positive rate would lead to a shortest path problem as explained in Section V-D. As expected, Figure 8 confirms that MSPC is activated more often when a higher true positive rate is desired.

The power consumption of our decision making module can be compared with that of an MSP430 microcontroller which consumes 3 mW in active mode. Figure 9 shows the amount of power savings obtained by our system compared to a system with the microcontroller being instantly active (a direct connection between node s and t in the screening graph). As expected, the higher the true positive rate is, the lower energy saving that can be achieved.

Once the optimal decision path is constructed, it can be used to measure its actual precision when test trials are applied. This simulates a real-time scenario where incoming signals are examined by the decision making module for identification of a specific target action. For this purpose, we fed the sensor data to the optimal decision paths shown in Table III. The actual measured true positive rates are shown in Figure 10. The values range from 56.7% to 100% with an average of 78.8%. We note that all values on the graph in Figure 10 are above the dashed line, which implies that the measured true positive rate is always higher than the desired lower bound (F).

E. Detecting Other Movements

In order to establish the robustness of our granular decision making architecture with respect to different target

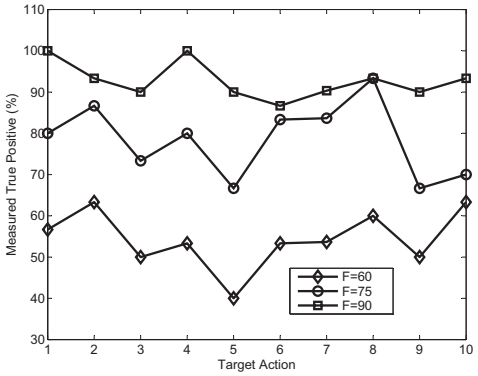

Figure 12. Measured sensitivity for detecting different movements. Results are shown for three values of desired true positive (60%, 75%, and 90%.).

actions, we used the data collected from our sensing platform and considered each action in Table II to be the target action. In each case, appropriate template was chosen and the specific action was considered as the target. For each target action, the optimal decision path was constructed from the screening graph as discussed in Section V. For extracting each decision path, the thresholds were set on each template matching block to meet the desired true positive rate. The sequence of the screening blocks on the decision path was used to accept/reject each incoming signal and activate MSPC. The set of screening blocks were then employed to classify the target movement. The results obtained from this analysis are shown in Figure 11 and Figure 12 for three different sensitivity rates. In particular, our system achieves an average power saving of 65.2% while maintaining a true positive rate of 92.7%.

VII. Discussion and Future Work

The power consumption of our granular decision making module is six orders of magnitude smaller than state-of-the-art low-power microcontrollers.

The amount of power savings that can be achieved by our decision making architecture highly depends on the frequency of occurrence of the target action. For our experiments, we assumed that all actions are equally likely, and therefore, 'sit to stand' occurs 10% of the times. In reality, however, human actions are sparse occurring much less frequently, which results in much higher power savings.

In our experiments, we used only a single sensor (Z-axis of accelerometer on 'waist' node) to detect target actions. In general, there might be actions that require information from multiple sensors. In such cases, the designer can replicate the granular decision making to accept/reject each incoming action. The microcontroller can be activated based on the decision made by a decision fusion module. The data fusion from multiple sensor nodes is out of scope of this paper and is the subject of our future work.

In this paper, we focused on optimizing screening path with respect to bit resolution. In future, we will also investigate the effect of other tuning parameters such as sampling rate and window size on the accuracy and the complexity of the signal processing as well as the energy saving.

VIII. Conclusion

We proposed a light-weight signal processing methodology for Body Sensor Networks applications by early rejection of non-target action. The proposed hardware-assisted algorithm uses template matching blocks at different bit levels and finds an optimal order for their execution. Our experimental results demonstrate the effectiveness of the proposed architecture in reducing the power consumption of the system. In particular, we achieved an energy saving of 65.2% while maintaining 92.7% true positive rates in detecting actions of interest.

References

[1] S. L. Mitchell, J. J. Collin, C. J. D. Luca, A. Burrows, and L. A. Lipsitz, "Open-loop and closed-loop postural control mechanisms in parkinson's disease: increased mediolateral activity during quiet standing," *Neuroscience Letters*, vol. 197, no. 2, pp. 133 – 136, 1995.

[2] S. Morris and J. Paradiso, "Shoe-integrated sensor system for wireless gait analysis and real-time feedback," *[Engineering in Medicine and Biology, 2002. 24th Annual Conference and the Annual Fall Meeting of the Biomedical Engineering Society] EMBS/BMES Conference, 2002. Proceedings of the Second Joint*, vol. 3, pp. 2468–2469 vol.3, Oct. 2002.

[3] P. Cuddihy, J. Weisenberg, C. Graichen, and M. Ganesh, "Algorithm to automatically detect abnormally long periods of inactivity in a home," in *Proceedings of the 1st ACM SIGMOBILE international workshop on Systems and networking support for healthcare and assisted living environments*. ACM, 2007, p. 94.

[4] K. Stangel, S. Kolnsberg, D. Hammerschmidt, B. Hosticka, H. Trieu, and W. Mokwa, "A programmable intraocular cmos pressure sensor system implant," *IEEE Journal of Solid-State Circuits*, vol. 36, no. 7, pp. 1094–1100, 2001.

[5] W.-S. Liew, L. Zou, X. abd Yao, and Y. Lian, "A 1-v 60-uw 16-channel interface chip for implantable neural recording," in *Proceedings of the Custom Integrated Circuits Conference*, 2009, pp. 507–510.

[6] S. Sasaki, T. Seki, and S. Sugiyama, "Batteryless accelerometer using power feeding system of rfid," in *2006 SICE-ICASE International Joint Conference*, 2006, pp. 3567–3570.

[7] A. Shoeb, D. Carlson, E. Panken, and T. Denison, "A micropower support vector machine based seizure de-

tection architecture for embedded medical devices," in *Proceedings of the 31st Annual International Conference of the IEEE Engineering in Medicine and Biology Society: Engineering the Future of Biomedicine, EMBC 2009*, 2009, pp. 4202–4205.

[8] P. Cong, N. Chaimanonart, W. Ko, and D. Young, "A wireless and batteryless 10-bit implantable blood pressure sensing microsystem with adaptive rf powering for real-time laboratory mice monitoring," *IEEE Journal of Solid-State Circuits*, vol. 44, no. 12, pp. 3631–3644, 2009.

[9] N. Chaimanonart and D. Young, "A wireless batteryless in vivo ekg and body temperature sensing microsystem with adaptive rf powering for genetically engineered mice monitoring," 2009, pp. 1473–1476.

[10] P. Cong, W. Ko, and D. Young, "Wireless batteryless implantable blood pressure monitoring microsystem for small laboratory animals," *IEEE Sensors Journal*, vol. 10, no. 2, pp. 243–254, 2010.

[11] P. Cong, N. Chaimanonart, W. Ko, and D. Young, "A wireless and batteryless 130mg 300μw 10b implantable blood-pressure-sensing microsystem for real-time genetically engineered mice monitoring," in *Solid-State Circuits Conference - Digest of Technical Papers, 2009. ISSCC 2009. IEEE International*, 2009, pp. 428 –429,429a.

[12] J. Parramon, P. Doguet, D. Marin, M. Verleyssen, R. Munoz, L. Leija, and E. Valderrama, "Asic-based batteryless implantable telemetry microsystem for recording purposes," in *Annual International Conference of the IEEE Engineering in Medicine and Biology - Proceedings*, vol. 5, 1997, pp. 2225–2228.

[13] N. Najafi and A. Ludomirsky, "Initial animal studies of a wireless, batteryless, mems implant for cardiovascular applications," *Biomedical Microdevices*, vol. 6, no. 1, pp. 61–65, 2004.

[14] T. Douseki, "Ultralow-voltage mtcmos/soi technology for batteryless mobile system," in *International Conference on Solid-State and Integrated Circuits Technology Proceedings, ICSICT*, vol. 2, 2004, pp. 1242–1247.

[15] T. Douseki, T. Tsukahara, Y. Yoshida, F. Utsunomiya, and N. Hama, "A batteryless wireless system with mtcmos/soi circuit technology," in *Proceedings of the Custom Integrated Circuits Conference*, 2003, pp. 163–168.

[16] L. Chao, C.-Y. Tsui, and W.-H. Ki, "A batteryless vibration-based energy harvesting system for ultra low power ubiquitous applications," in *Proceedings - IEEE International Symposium on Circuits and Systems*, 2007, pp. 1349–1352.

[17] H. Ghasemzadeh, V. Loseu, and R. Jafari, "Structural action recognition in body sensor networks: Distributed classification based on string matching," *IEEE Transactions on Information Technology in Biomedicine*, vol. 14, no. 2, pp. 425–435, 2010.

[18] J. Polastre, R. Szewczyk, and D. Culler, "Telos: enabling ultra-low power wireless research," *Information Processing in Sensor Networks, 2005. IPSN 2005. Fourth International Symposium on*, pp. 364–369, April 2005.

[19] H. Ghasemzadeh and R. Jafari, "Energy-efficient buffer allocation in light-weight embedded systems: A greedy convex optimization," in *The International Conference on Hardware-Software Codesign and System Synthesis (CODES+ISSS)*, 2010.

[20] G. Yang and M. Yacoub, *Body sensor networks*. Springer-Verlag New York Inc, 2006.

[21] H. Ghasemzadeh, E. Guenterberg, and R. Jafari, "Energy-Efficient Information-Driven Coverage for Physical Movement Monitoring in Body Sensor Networks," *IEEE Journal on Selected Areas in Communications*, vol. 27, pp. 58–69, 2009.

[22] R. O. Duda, P. E. Hart, and D. G. Stork, *Pattern Classification*. Wiley-Interscience Publication, 2000.

[23] S. Patel, K. Lorincz, R. Hughes, N. Huggins, J. Growdon, M. Welsh, and P. Bonato, "Analysis of feature space for monitoring persons with Parkinson's Disease with application to a wireless wearable sensor system," in *Engineering in Medicine and Biology Society, 2007. EMBS 2007. 29th Annual International Conference of the IEEE*. IEEE, 2007, pp. 6290–6293.

[24] M. Ohayon and T. Roth, "Prevalence of restless legs syndrome and periodic limb movement disorder in the general population," *Journal of psychosomatic research*, vol. 53, no. 1, pp. 547–554, 2002.

[25] H. Ghasemzadeh, J. Barnes, E. Guenterberg, and R. Jafari, "A Phonological Expression for Physical Movement Monitoring in Body Sensor Networks," in *Mobile Ad Hoc and Sensor Systems, 2008. MASS 2008. 5th IEEE International Conference on*, 2008, pp. 58–68.

[26] Z. Yang, "Fast template matching based on normalized cross correlation with centroid bounding," in *Measuring Technology and Mechatronics Automation (ICMTMA), 2010 International Conference on*, vol. 2, 13-14 2010, pp. 224 –227.

[27] A. Sen, K. Candan, A. Ferreira, B. Beauquier, and S. Perennes, "On shortest path problems with non-Markovian link contribution to path lengths," *Networking 2000 Broadband Communications, High Performance Networking, and Performance of Communication Networks*, pp. 859–870, 2000.

[28] E. Moore, "The shortest path through a maze," in *Proceedings of the International Symposium on the Theory of Switching*, vol. 2, 1959, pp. 285–292.